Applied Magnetic Resonance (2023) 54:449–461
https://doi.org/10.1007/s00723-022-01510-x

Applied
Magnetic Resonance

ORIGINAL PAPER

Magnetic Properties of $La_{0.81}Sr_{0.19}Mn_{0.9}Fe_{0.1-x}Zn_xO_3$ ($x=0$, $x=0.05$)

R. M. Eremina[1] · I. V. Yatsyk[1] · Z. Y. Seidov[2] · F. G. Vagizov[3] · V. A. Shustov[1] · A. G. Badelin[4] · V. K. Karpasyuk[4] · D. S. Abdinov[2] · M. M. Tagiev[5] · S. Kh. Estemirova[6] · H.-A. Krug von Nidda[7]

Received: 29 July 2022 / Revised: 18 October 2022 / Accepted: 26 October 2022 /
Published online: 7 November 2022

Abstract

Magnetic properties of polycrystalline $La_{0.81}Sr_{0.19}Mn_{0.9}Fe_{0.1-x}Zn_xO_3$ ($x=0$, 0.05) have been investigated by means of electron spin resonance, magnetic susceptibility, and Mössbauer measurements. Both samples show a clear ferromagnetic transition. The Curie temperature T_C decreases on increasing Fe content ($x=0.05$—$T_C=222$ K; $x=0$—$T_C=148$ K). Mössbauer studies indicate that Fe in these compounds is in the trivalent high-spin state. The temperature evolution of the Mössbauer spectra at low temperatures ($T<T_C$) is typical for ferromagnetic clusters with a wide distribution in size and magnetic correlation length. The inverse susceptibility of all the samples deviates from the Curie–Weiss law above T_C, indicating the presence of fluctuations on approaching magnetic order. An anomalous downturn of the inverse susceptibility for $x=0.05$ significantly above T_C and the concomitant observation of ferromagnetic resonance signals coexisting with the paramagnetic resonance up to approximately room temperature, is caused by a Griffiths-like behavior. This regime is characterized by the coexistence of ferromagnetic entities within the globally paramagnetic phase.

✉ Z. Y. Seidov
zsyu@rambler.ru

[1] Zavoisky Physical-Technical Institute, Federal Research "Kazan Scientific Center of RAS", Kazan 420029, Russia

[2] Institute of Physics, Azerbaijan National Academy of Sciences, Baku AZ1143, Azerbaijan

[3] Institute of Physics, Kazan Federal University, Kazan 420008, Russia

[4] Astrakhan State University, Astrakhan 414056, Russia

[5] Azerbaijan State University of Economics, Baku AZ1001, Azerbaijan

[6] Institute for Metallurgy, Ural Division of RAS, Yekaterinburg 620016, Russia

[7] Experimental Physics V, EKM, Institute of Physics, University of Augsburg, 6135 Augsburg, Germany

1 Introduction

$La_{1-X}A_XMn_{1-Y}Fe_YO_3$ (A=Ca, Sr) belongs to the family of hole-doped mixed valence manganite perovskites, exhibiting a colossal magnetoresistance (CMR) and magnetocaloric effect [1–4]. The hole doping of manganite perovskites, realized by substitution of a divalent element for La^{3+} or by formation of cation vacancies, results in a fraction of Mn^{4+} ions on the Mn^{3+} sites [5]. The $Mn^{3+;4+}$ mixed valence leads to ferromagnetic (FM) Mn^{3+}–Mn^{4+} double-exchange (DE) interactions, competing with antiferromagnetic (AFM) Mn^{3+}–Mn^{3+} super-exchange (SE) interactions [5]. The case of Fe substitution is particularly interesting because of the large extent to which it can replace Mn due to similar ionic radii of Fe^{3+} and Mn^{3+}. The magnetic investigations of $La_{1-x}Sr_xMn_{1-y}Fe_yO_3$ (with x=0.3 and y=0.15–0.25) and $La_{1-x}Ca_xMn_{1-y}Fe_yO_3$ (with x=0.37 and y=0–0.18) show that in both systems the FM Curie temperature T_C decreases with increasing y [2, 4]. Such behavior of the transition temperature T_C is connected with the weakening of the double-exchange FM interaction by Fe doping [2, 4, 6]. In this article, we present X-ray diffraction, magnetization, electron spin resonance (ESR), and Mössbauer experiments on polycrystalline samples of $La_{0.81}Sr_{0.19}Mn_{0.9}Fe_{0.05}Zn_{0.05}O_3$ and $La_{0.81}Sr_{0.19}Mn_{0.9}Fe_{0.1}O_3$. Notably, our previous results on polycrystalline $La_{0.83}Sr_{0.17}Mn_{0.9}Fe_{0.1-x}Zn_xO_3$ (x=0, 0.05) [6] indicate the important role of magnetic cluster formation both in the FM ordered and in the paramagnetic (PM) phase. Especially in the latter one, the Griffiths phase can be tuned by the balance of disorder (Zn^{2+}) and AFM interactions (Fe^{3+}).

2 Sample Preparation and Characterization

Polycrystalline samples of $La_{0.81}{}^{3+}Sr_{0.19}{}^{2+}Mn_{0.71-x}{}^{3+}Mn_{0.19+x}{}^{4+}Fe_{0.1-\times}{}^{3+}Zn_x{}^{2+}O_3{}^{2-}$ with x=0 and x=0.05 were synthesized by traditional ceramic processing, including two grindings in a ball mill with addition of alcohol and preliminary burning at 1273 K for 4 h. The final sintering step was performed in air at 1473 K for 10 h, and the samples were cooled together with the furnace. To provide stoichiometric oxygen content, the samples were annealed at 1223 K and partial pressure of oxygen in the gas phase $p_{O_2}=10^{-1}$ Pa. The choice of annealing conditions was based on the data of Ref. [7]. Annealing was carried out for 96 h. Phase composition and unit-cell parameters were determined by powder X-ray diffraction at room temperature (diffractometer Shimadzu XRD-7000, CuK_α radiation). The X-ray diffraction analysis of the synthesized manganites x=0 and x=0.05 showed that both compounds belong to the proper space group $R\bar{3}c$. The corresponding unit-cell parameters, presented in Table 1, were determined and refined using the Maud-v2.94 program package [6, 8, 9].

Table 1 Crystallographic data for $La_{0.83}Sr_{0.17}Mn_{0.9}Fe_{0.05}Zn_{0.05}O_3$ and $La_{0.83}Sr_{0.17}Mn_{0.9}Fe_{0.1}O_3$

Compound	Cryst. str	a (Å)	c (Å)	α (°)	β (°)	γ (°)
$La_{0.81}Sr_{0.19}Mn_{0.9}Fe_{0.05}Zn_{0.05}O_3$	Trig.($R\,\bar{3}\,c$)	5.5302	13.3655	90	90	120
$La_{0.81}Sr_{0.19}Mn_{0.9}Fe_{0.1}O_3$	Trig.($R\,\bar{3}\,c$)	5.5268	13.3643	90	90	120

3 Results and Discussion

3.1 Magnetic Susceptibility and Magnetization

Magnetization measurements were performed using a superconducting quantum interference device (SQUID) magnetometer MPMS5 (Quantum Design) in magnetic fields up to $H \leq 50$ kOe for the temperature regime $1.8 \leq T \leq 400$ K. Figures 1 and 2 show the temperature dependence of the magnetic susceptibility and its inverse for the compounds $La_{0.81}Sr_{0.19}Mn_{0.9}Fe_{0.1-x}Zn_xO_3$ ($x = 0,\ 0.05$). The Curie temperature T_C, defined as the one corresponding to the peak of $d\chi/dT$ in the χ vs T curve (see insets in Figs. 1 and 2), amounts to T_C ($x = 0.05$) = 222 K and T_C ($x = 0$) = 148 K, respectively (Table 2). The temperature dependence of the inverse susceptibility $\chi^{-1}(T)$ measured in different magnetic fields for the compound $x = 0.05$ is shown in the lower frame of Fig. 1. For $H = 10$ kOe at high T, $\chi^{-1}(T)$ varies linearly with T indicating a Curie–Weiss (CW) behavior. However, for the measurements done in lower dc fields (100 and 1000 Oe), $\chi^{-1}(T)$ shows a

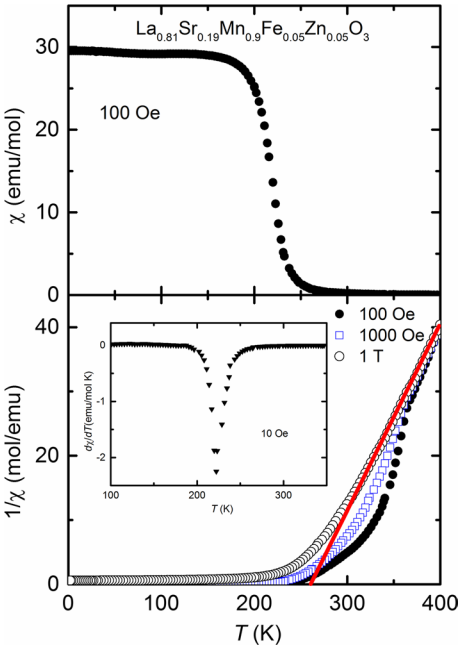

Fig. 1 Temperature dependence of dc magnetic susceptibility (upper frame) at $H = 100$ Oe and its inverse (lower frame) in $La_{0.81}Sr_{0.19}Mn_{0.9}Fe_{0.05}Zn_{0.05}O_3$ at 100 Oe, 1000 Oe, and 10 kOe. The solid line indicates a fit by a Curie–Weiss law. Inset (lower frame): The derivative of magnetic susceptibility $d\chi/dT$ as a function of temperature

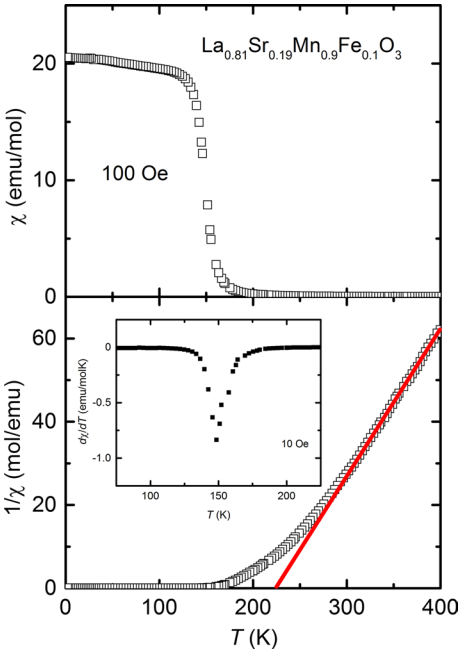

Fig. 2 Temperature dependence of dc magnetic susceptibility (upper frame) and its inverse (lower frame) in $La_{0.81}Sr_{0.19}Mn_{0.9}Fe_{0.1}O_3$ at $H = 100$ Oe. The solid line indicates a fit by a Curie–Weiss law. Inset (lower frame): the derivative of magnetic susceptibility $d\chi/dT$ as a function of temperature

Table 2 Magnetization M at 2 K (in μ_B per formula unit), paramagnetic Curie–Weiss temperature Θ_{CW} (K), magnetic ordering temperature T_C and effective paramagnetic moment μ_{eff}(μ_B/f.u.) in $La_{0.81}Sr_{0.19}Mn_{0.9}Fe_{0.1-x}Zn_xO_3$ ($x = 0, 0.05$)

Compounds	M_s (μ_B/f.u.) at 2 K	Θ_{CW} (K)	T_C (K)	μ_{eff} (μ_B/f.u.)
$La_{0.81}Sr_{0.19}Mn_{0.9}Fe_{0.05}Zn_{0.05}O_3$	3.038	260	222	5.305
$La_{0.81}Sr_{0.19}Mn_{0.9}Fe_{0.1}O_3$	2.363	225	148	4.749

downward deviation from linearity below a temperature $T_G \sim 364$ K, significantly above T_C, which turns out to be the stronger the smaller the external field and is a typical signature of a Griffiths phase [10–17], where FM clusters coexist in the PM matrix. As the applied external magnetic field increases, the extent of deviation in magnetic susceptibility systematically diminishes until a pure CW behavior is observed. This is related to the fact that the magnetization of the PM matrix increases linearly with increasing H [10, 11, 17], while the contribution of the FM clusters is saturated already in small fields and, hence, for a sufficiently high field, the PM susceptibility dominates over the weakly correlated FM clusters. The effective moment determined from the CW law as $\mu_{eff} = 5.305\mu_B$ is strongly enhanced compared to the theoretical value of $4.6\mu_B$ calculated from the square root of the sum of squared ionic moments of Mn^{3+}($S = 2$), Mn^{4+} ($S = 3/2$), and Fe^{3+} ($S = 5/2$) weighted by the corresponding stoichiometric factors and using the spin-only g value $g = 2$ [17]. This observation corroborates the general tendency for FM cluster formation in the PM phase in this compound.

Compared to $x=0.05$, the $\chi^{-1}(T)$ curve of the Zn-free compound $x=0$ (Fig. 2) does not exhibit any obvious downturn deviation from the CW law which could be a signature of a Griffiths phase. Note that the deviation to higher values from linearity below a certain temperature above T_C is due to fluctuations characteristic of usual ferromagnets. The effective moment determined from the CW law as $\mu_{eff}=4.749\mu_B$ approximately matches the theoretical value of $4.834\mu_B$. Thus, in the PM phase, the tendency for FM cluster formation is significantly weaker for $x=0$ than for $x=0.05$.

Figure 3 shows the magnetization of $La_{0.81}Sr_{0.19}Mn_{0.9}Fe_{0.1-x}Zn_xO_3$ ($x=0$, 0.05) as a function of magnetic field at 2 K. The magnetization of the compound $x=0.05$ reveals practically no hysteresis and immediately reaches the full saturation value at weak external fields. For $x=0$, one observes a weak hysteresis and, above 15 kOe, the magnetization still slightly increases on increasing magnetic field. The saturation magnetization (M_S) in both compounds was obtained from a linear extrapolation of the high-field data [6, 18] as function of the inverse magnetic field down to $1/H=0$ as illustrated in the left inset of Fig. 3 and the values of M_S ($T=2$ K) are deduced as $3.049\mu_B$ and $2.409\mu_B$, to be compared to the theoretical values $3.11\mu_B$ and $2.91\mu_B$, respectively, which are calculated assuming $g=2$ for all magnetic ions and antiparallel alignment of the Fe ions with respect to the Mn ions. While the theoretical value for $x=0.05$ is in fair agreement with the experimental value, it is overestimated for $x=0$. This is probably due to the fact that the linear extrapolation of M vs $1/H$ is not applicable here, because of the non-zero curvature of the data.

3.2 Electron Spin Resonance

To further identify the presence of a Griffiths phase, we performed electron spin resonance (ESR) measurements on the $La_{0.81}Sr_{0.19}Mn_{0.9}Fe_{0.05}Zn_{0.05}O_3$ and

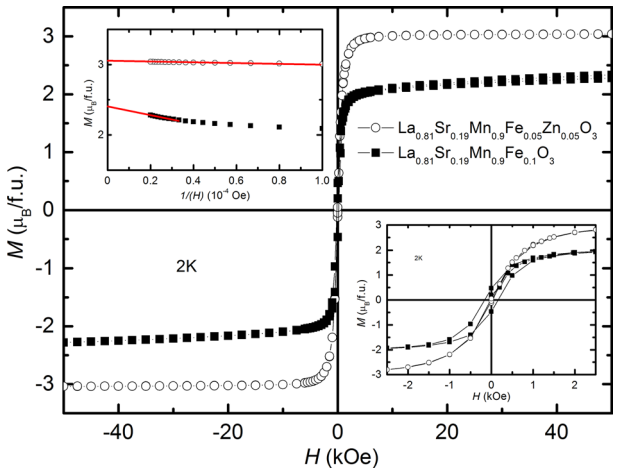

Fig. 3 Magnetization as a function of external field in $La_{0.81}Sr_{0.19}Mn_{0.9}Fe_{0.05}Zn_{0.05}O_3$ and $La_{0.81}Sr_{0.19}Mn_{0.9}Fe_{0.1}O_3$ measured at 2 K. Right inset: magnification at low fields. Left inset: magnetization as function of inverse field to determine the saturation magnetization

$La_{0.81}Sr_{0.19}Mn_{0.9}Fe_{0.1}O_3$ samples. ESR is known as a powerful probe of spin dynamics and magnetic correlation in magnetic materials on a microscopic level. The signal of ESR is sensitive to the variation of localized environment of magnetic ions. Due to this feature, ESR has been also applied to identify the existence of Griffiths phases in some manganites previously [10–12, 19–23]. The ESR measurements have been performed using a BRUKER EMXplus spectrometer working at X-band frequency (9.4 GHz) and equipped with a nitrogen gas-flow cryostat. Due to the lock-in technique with field modulation, the field derivative of the absorbed microwave power (d*P*/d*H*) is recorded as a function of the externally applied field. The observed ESR spectra of $La_{0.81}Sr_{0.19}Mn_{0.9}Fe_{0.05}Zn_{0.05}O_3$ and $La_{0.81}Sr_{0.19}Mn_{0.9}Fe_{0.1}O_3$ are shown in Figs. 4 and 5, respectively.

Figure 4 depicts a series of ESR spectra in a temperature range from 215 to 320 K across the phase-transition regime (near and above T_C) for $La_{0.81}Sr_{0.19}Mn_{0.9}Fe_{0.05}Zn_{0.05}O_3$. At $T \geq 300$ K only a single PM resonance line shows up corresponding to the paramagnetic state. But at lower temperatures, the spectra do not only consist of a PM signal due to the majority of Mn^{3+}–Mn^{4+} spins, but also exhibit an intriguing FMR signal at lower resonance fields. Compared to PM resonance lines, the extra peak shows a notable difference which is strongly dependent on temperature. As shown in the left and right part of Fig. 4, with the decrease of temperature, the intensity of this peak does not only increase but also the peak position gradually moves towards lower magnetic field. Therefore, from 300 K down to 220 K, two peaks coexist indicating that two different magnetic phases coexist in the system. At $T = 215$ K, both peaks finally merge into a single broad peak, which further shifts to lower field region. In Fig. 1, at $T < 220$ K, one recognizes that the sample has undergone the PM–FM phase transition and all PM phase completely turns into the FM phase. Consequently, at $T < 220$ K, there remains only a single FMR peak to be detected. Thus, the

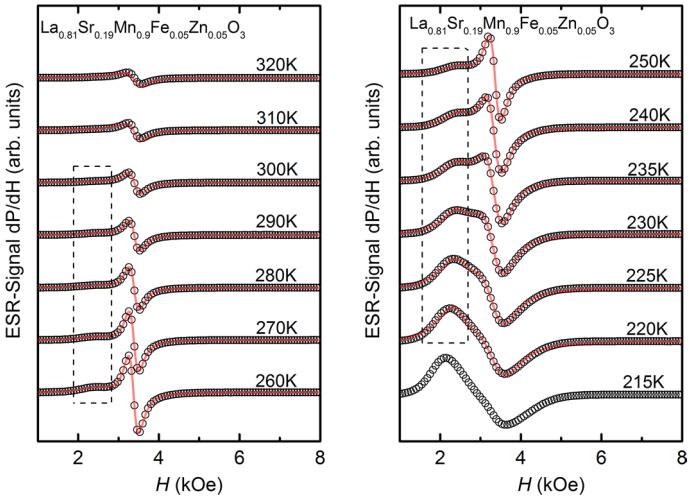

Fig. 4 ESR spectra of $La_{0.81}Sr_{0.19}Mn_{0.9}Fe_{0.05}Zn_{0.05}O_3$ at temperatures $215 \leq T \leq 320$ K

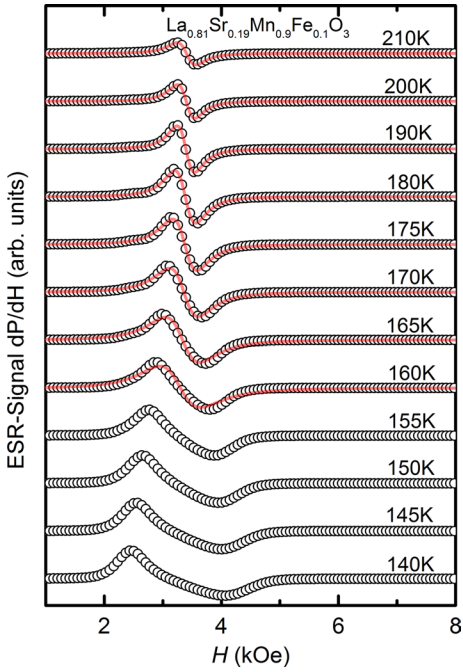

Fig. 5 ESR spectra of $La_{0.81}Sr_{0.19}Mn_{0.9}Fe_{0.1}O_3$ at temperatures $140 \leq T \leq 210$ K

temperature regime of coexisting ESR signals is in fair agreement with the GP regime derived from the susceptibility data.

For $La_{0.81}Sr_{0.19}Mn_{0.9}Fe_{0.1}O_3$, we observed a typical paramagnetic resonance line with a g-factor of approximately 2 in the temperature range $T > 160$ K, which is slightly higher than the onset temperature of the PM–FM transition in $\chi^{-1}(T)$ (cf. Figure 2). To lower temperature, distortions of the resonance line show up on crossing T_C and the signal exhibits the characteristic shape of FMR in a polycrystalline sample. The FMR shifts to lower field with decreasing temperature. Thus, the results of both $\chi^{-1}(T)$ and ESR show the normal PM–FM transition for $La_{0.81}Sr_{0.19}Mn_{0.9}Fe_{0.1}O_3$.

The full temperature dependences of the resonance fields H_{res} and linewidth data ΔH are summarized in Fig. 6. For $x = 0.05$, the splitting of the resonance fields is another key parameter for characterization of the coexistence of magnetic phases. The open and solid circles depict the temperature dependence of the resonance fields for PM and FM peak, respectively. One can see that the position of the PM peak is almost constant at a magnetic field of $H = 3386$ Oe showing only a weak temperature dependence. The FM resonance field can be resolved at about 3 kOe at 300 K and gradually shifts to lower fields on decreasing temperature. That the FM peak cannot be resolved up to $T_G \sim 364$ K, may be related to the fact that the precondition for the appearance of a well-defined FMR line is the formation of plate-like FM clusters, which is not necessarily fulfilled directly at the onset of the GP. Above the Curie temperature T_C, the linewidth ΔH of the PM line exhibits a minimum value of 210 Oe at a temperature of 270 K, diverges to lower temperature and increases

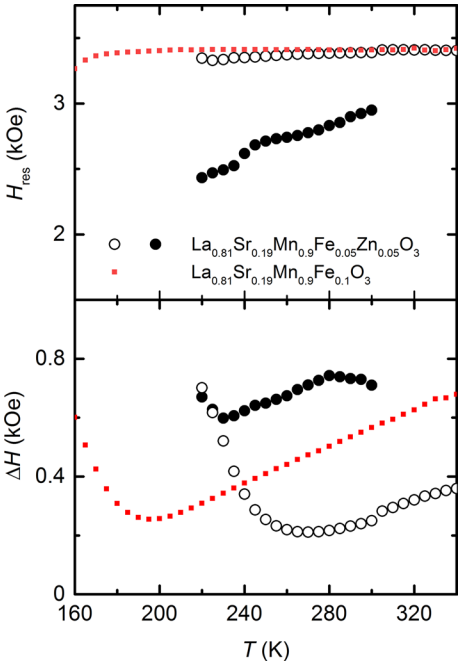

Fig. 6 Black open and closed circles-Temperature dependencies of the resonance field H_{res} and linewidth ΔH in $La_{0.81}Sr_{0.19}Mn_{0.9}Fe_{0.05}Zn_{0.05}O_3$. Red square -Temperature dependence of the resonance field H_{res} and linewidth ΔH in $La_{0.81}Sr_{0.19}Mn_{0.9}Fe_{0.1}O_3$

approximately with linear slope (characteristic for relaxation via spin-phonon coupling [24]) to higher temperature, whereas ΔH of the FMR slightly increases with temperature and then decreases on approaching T_G. For $x=0$, the temperature dependences of resonance field and linewidth of the PM peak show a similar behavior above T_C like for $x=0.05$.

Thus, the ESR results support the findings of the magnetization measurements, i.e. for both compounds, one observes the typical behavior of the PM resonance on approaching a FM transition with resonance shift and line broadening due to enhanced internal demagnetization fields and critical fluctuations. For $x=0.05$, the additional FMR line corroborates the coexistence of a FM phase in the PM regime. Zn^{2+} substitution enhances the number of Mn^{4+} spins and in turn FM Mn^{3+}–Mn^{4+} DE, and at the same time, it increases disorder. Both effects favor the formation of a GP.

3.3 Mössbauer Effect Study

The Mössbauer measurements were carried out in a wide temperature range from room temperature to liquid nitrogen and liquid helium temperatures. The Mössbauer spectra of $La_{0.81}Sr_{0.19}Mn_{0.9}Fe_{0.05}Zn_{0.05}O_3$ at different temperatures are shown in Fig. 7. At room temperature, the Mössbauer spectrum consists of a slightly asymmetric doublet with a distribution of isomer (IS) and quadrupole shifts (QS). In the insets of Fig. 7, the distribution functions of the Mössbauer parameters are given. They were restored by processing the experimental spectra with the SpectrRelax

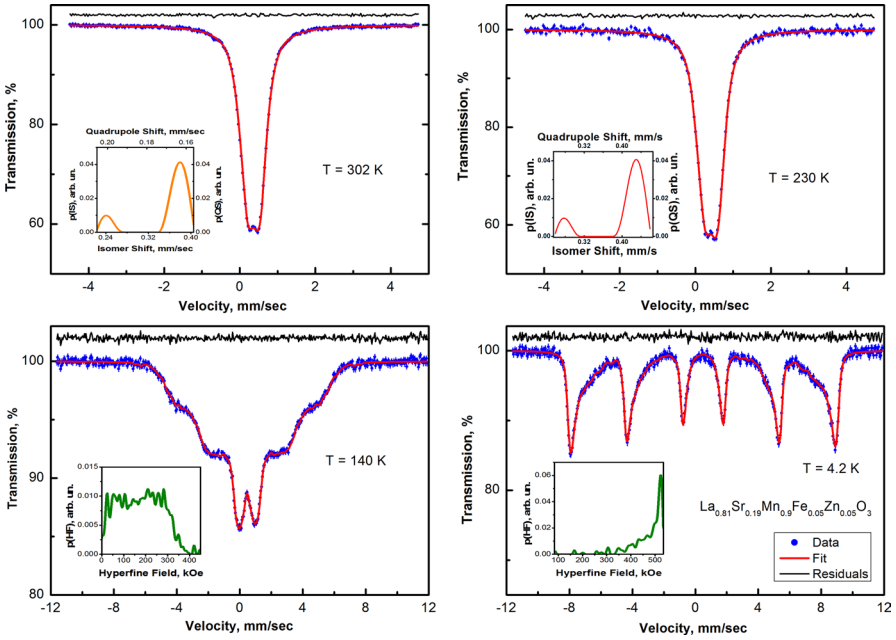

Fig. 7 Mössbauer spectra of $La_{0.81}Sr_{0.19}Mn_{0.9}Fe_{0.05}Zn_{0.05}O_3$ at temperatures 302 K, 230 K, 140 K, and 4.2 K; the difference between the experimental and approximating spectra in the range $\pm 3\sigma$ is shown above. Insets show the reconstructed distribution functions of IS, QS (300 K, 230 K) and hyperfine parameters (140 K, 4.2 K)

software [25]. At 300 K, the distribution function of Mössbauer parameters shows the presence of two well-defined centers of iron ions (with and without another iron ion as nearest neighbor) with an area ratio close to 1:5 at room temperature.

As it is known, the isomer shift reflects the density of s-electrons in the iron nucleus, and it is sensitive to the oxidation state of iron and the coordination number. The average values of the isomer and quadrupole shift of Fe nuclei in the studied sample are found as 0.35 mm/s and 0.17 mm/s, respectively. These values of the hyperfine parameters are typical for Fe^{3+} ions in the high-spin state, $(t^3_{2g}e^2_g)$ [26, 27]. Also, hyperfine parameters determined at low temperature are in good agreement with the data reported in the literature for similar compounds [28, 29].

The substitution of La by a divalent cation, Sr, results partly in a change of the Mn valence from 3+ to 4+ [28], so that a part of Mn^{3+} is transformed into Mn^{4+}. In this case, it is reasonable to expect the manifestation of the presence of Fe^{4+} ions in the room-temperature Mössbauer spectra in the form of absorption features in the region of low and negative velocities. As can be seen from the distribution function for the isomer shift in Fig. 7, in this velocity region, the features due to Fe^{4+} ions are not observed. Probably, the preferable substitution of Fe^{3+} ions for Mn^{3+} ions is due to the identical ion size of these elements in the high-spin state. When the temperature decreases, the Mössbauer spectra remain practically the same above T_C, but change dramatically in the magnetically ordered phase, first acquiring the form of relaxation spectra with a wide distribution of hyperfine magnetic fields up to 300

kOe, and then, in the temperature range of liquid helium, the Mössbauer spectra are transformed into magnetic sextets (Fig. 7, bottom frame). At a temperature of 4.2 K, a noticeable peak is observed in the distribution of hyperfine fields at a value of 520 kOe and an extended tail towards low fields (bottom inset in Fig. 7). Note that the Griffiths phase cannot be distinguished from a purely paramagnetic phase by means of Moessbauer spectroscopy, due to the fact that the volume fraction of the ferromagnetic clusters is less than 1% of the paramagnetic fraction, as has been shown earlier by Deisenhofer et al. [10], and hence cannot be resolved by Moessbauer spectroscopy.

The dependence of the mean hyperfine magnetic field on the temperature is given in Fig. 8a. According to the Mössbauer measurements, magnetic ordering of the iron ions is achieved at a temperature of 200 K for $La_{0.81}Sr_{0.19}Mn_{0.9}Fe_{0.05}Zn_{0.05}O_3$. The changes observed in the dependence of the mean quadrupole shift, ε, on temperature, also indicate the magnetic ordering of the iron ions (cf. Fig. 8b). When an ion is in a paramagnetic state, the splitting ΔE_Q between the lines of the quadrupole doublet is determined by the product of the electric field gradient (EFG) q at the nucleus and the quadrupole moment Q of the nucleus, i.e. $\Delta E_Q \approx 2\varepsilon = e^2qQ/2$. In the case of magnetic ordering of resonant atoms and the appearance of a hyperfine magnetic field on the nucleus oriented with respect to the direction of the main axis of the quadrupole interaction tensor at some angle θ, the quadrupole shift ε is determined by the expression: $\varepsilon = e^2qQ(3\cos^2\theta - 1)/8$. The sharp jump of the quadrupole shift observed in the region of the magnetic ordering temperature is probably due

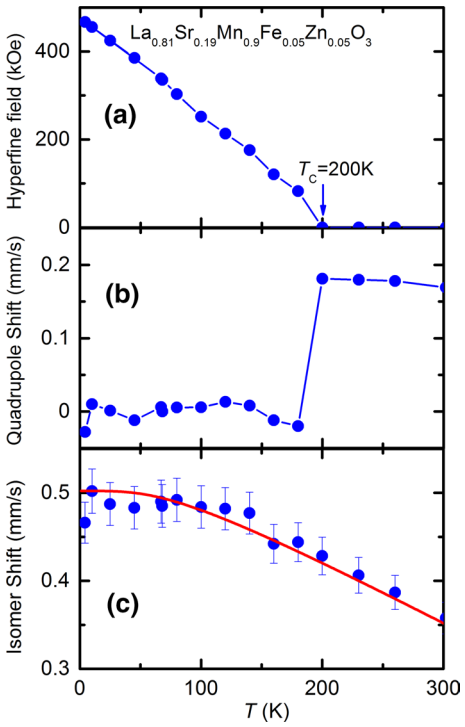

Fig. 8 Temperature dependence of Mössbauer parameters of ^{57}Fe in $La_{0.81}Sr_{0.19}Mn_{0.9}Fe_{0.05}Zn_{0.05}O_3$: **a** the average hyperfine magnetic field on the iron nuclei. **b** The average quadrupole shift, ε, **c** the average isomer shift, δ, of the iron nuclei

to the appearance of a hyperfine magnetic field on the nucleus at some angle to the direction of the EFG. The temperature dependence of the average isomer shift of iron ions presented in Fig. 8c, is mainly determined by the second-order Doppler effect. Its value decreases monotonically with increasing temperature. The solid line shows a curve that approximates, in the Debye approximation, the experimental values of the average isomer shift.

It should be noted that the relaxation-like shape of the Mössbauer spectra and the specific temperature dependence of the average hyperfine field on the iron nuclei, which are unusual for conventional magnetically ordered materials, suggest that at low temperatures, a complex magnetic correlation is formed in the samples under study.

4 Conclusions

In summary, we have investigated the magnetic behavior of polycrystalline samples of $La_{0.81}Sr_{0.19}Mn_{0.9}Fe_{0.1-x}Zn_xO_3$ ($x=0$, 0.05). All samples show a clear FM-PM transition at T_C. The downward deviation of PM magnetization data from the CW law together with the FMR line coexisting with the PM ESR signal suggests that the GP model is appropriate to describe the short-range ordered state for $x=0.05$, while the upward deviation observed for $x=0$ is caused by conventional fluctuations on approaching magnetic order. Mössbauer measurements show that in the studied perovskite-like manganites, doping with iron ions leads to the replacement of Mn^{3+} ions by Fe^{3+} ions in the high-spin state with the same ionic radius. Consequently, Fe ions occupy Mn sites without significant lattice distortions. However, this tendency can lead to phase separation and the formation of various magnetic clusters embedded in the paramagnetic matrix. The observed temperature dependence of the Mössbauer spectra of the compounds under study is typical of ferromagnetic clusters with a wide size distribution and magnetic correlation length. The temperature evolution of the spectra is probably determined by fluctuations of the iron magnetic moments due to the competition between the thermal energy and the energy of magnetic correlation.

Supplementary Information The online version contains supplementary material available at https://doi.org/10.1007/s00723-022-01510-x.

Acknowledgements The authors thank Dana Vieweg for SQUID measurements.

Author Contributions RE and ZS: conceptualization, methodology, formal analysis, original draft preparation, writing—review and editing, supervision; FV: investigation by Mössbauer method, methodology, formal analysis, writing—original draft; IY: Investigation by ESR method, methodology, formal analysis; VS: investigation by X-ray method, methodology, formal analysis; AB, VK, and SE: sample synthesis, methodology, characterization; DA and MT: Resources, visualization; H-A KvN: project administration, investigation of the magnetization, writing—reviewing and editing. All authors have read and agreed to the published version of the manuscript.

Funding This work was partially supported by the Deutsche Forschungsgemeinschaft (DFG) within the Transregional Collaborative Research Center TRR 80 "From Electronic Correlations to Functionality", project no. 107745057 (Augsburg, Munich, Stuttgart). The work of Z.Y. Seidov, M.M. Tagiev and D.S.

Abdinov was supported by the Science Development Foundation under the President of the Republic Azerbaijan Grant EIF-BGM-4-RFTF-1/2017–21/03/1-M-03. Electron spin resonance measurements (I.V. Yatsyk, V.A. Shustov, R.M. Eremina) were performed with the financial support from the government assignment for FRC Kazan Scientific Center of RAS.

Data Availability Statement The data that were used and analyzed are presented in the article.

Declarations

Conflict of interest The authors declare that they have no known competing financial interests or personal relationships that could have appeared to influence the work reported in this paper.

References

1. Y. Tokura, Y. Tomioka, Colossal magnetoresistive manganites. J. Magn. Magn. Mater. **200**(1), 1–23 (1999). https://doi.org/10.1016/S0304-8853(99)00352-2
2. K. Ahn, X.W. Wu, K. Liu, C.L. Chien, Magnetic properties and colossal magnetoresistance of La(Ca)MnO_3 materials doped with Fe. Phys. Rev. B **54**(21), 15299 (1996). https://doi.org/10.1103/physrevb.54.15299
3. G. Wang, Z.R. Zhao, H.L. Li, X.F. Zhang, Magnetocaloric effect and critical behavior in Fe-doped $La_{0.67}Sr_{0.33}Mn_{1-x}Fe_xO_3$ manganites. Ceram. Int. **42**(16), 18196 (2016). https://doi.org/10.1016/j.ceramint.2016.08.138
4. V. Zakhvalinskii, R. Laiho, A.V. Lashkul, K.G. Lisunov, E. Lähderanta, Yu.S. Nekrasova, P.A. Petrenko, Phase separation, ferromagnetism and magnetic irreversibility in $La_{1-x}Sr_xMn_{1-y}Fe_yO_3$. J. Magn. Magn. Mater. **323**(16), 2186–2191 (2011). https://doi.org/10.1016/j.jmmm.2011.03.028
5. J. Coey, M. Viret, S. von Molnar, Mixed-valence manganites. Adv. Phys. **48**(2), 167 (1999). https://doi.org/10.1080/000187399243455
6. Z.Y. Seidov, I.V. Yatsyk, F.G. Vagizov, V.A. Shustov, A.G. Badelin, V.K. Karpasyuk, M.J. Najafzade, I.N. Ibrahimov, SKh. Estemirova, H.-A. Krug von Nidda, R.M. Eremina, Local magnetic properties of $La_{0.83}Sr_{0.17}Mn_{0.9}Fe_{0.1-x}Zn_xO_3$. J. Magn. Magn. Mater. **552**, 169190 (2022)
7. J. Mizusaki, N. Mori, H. Takai, Y. Yonemura, H. Minamiue, H. Tagawa, M. Dokiya, H. Inaba, K. Naraya, T. Sasamoto, T. Hashimotoand, Oxygen nonstoichiometry and defect equilibrium in the perovskite-type oxides $La_{1-x}Sr_xMnO_{3+d}$. Solid State Ionics **129**(1–4), 163–177 (2000). https://doi.org/10.1016/S0167-2738(99)00323-9
8. Maud, Materials analysis using diffraction. http://maud.radiographema.eu.
9. D. Popov, T.P. Gavrilova, I.F. Gilmutdinov, M.A. Cherosov, V.A. Shustov, E.M. Moshkina, L.N. Bezmaternykh, R.M. Eremina, Magnetic properties of ludwigite $Mn_{2.25}Co_{0.75}BO_5$. J. Phys. Chem. Solids **148**, 109695 (2021). https://doi.org/10.1016/j.jpcs.2020.109695
10. J. Deisenhofer, D. Braak, H.-A. Krug von Nidda, J. Hemberger, R.M. Eremina, V.A. Ivanshin, A.M. Balbashov, G. Jug, A. Loidl, T. Kimura, Y. Tokura, Observation of a Griffiths phase in paramagnetic $La_{1-x}Sr_xMnO_3$. Phys. Rev. Lett. **95**(12), 257202 (2005). https://doi.org/10.1103/PhysRevLett.95.257202
11. R. Eremina, I.I. Fazlizhanov, I.V. Yatsyk, K.R. Sharipov, A.V. Pyataev, H.-A. Krug von Nidda, N. Pascher, A. Loidl, K.V. Glazyrin, Y.M. Mukovskii, Phase separation in paramagnetic $Eu_{0.6}La_{0.4-x}Sr_xMnO_3$. Phys. Rev. B **84**(6), 064410 (2011). https://doi.org/10.1103/PhysRevB.84.064410
12. N. Rama, M.S. Ramachandra Rao, V. Sankaranarayanan, P. Majewski, S. Gepraegs, M. Opel, R. Gross, A-site-disorder-dependent percolative transport and Griffiths phase in doped manganites. Phys. Rev. B **70**(22), 224424 (2004). https://doi.org/10.1103/PhysRevB.70.224424
13. X. Zheng, T. Gao, W. Jing, X. Wang, Y. Liua, B. Chen, H. Dong, Z. Chen, S. Cao, C. Cai, V.V. Marchenkov, Evolution of Griffiths phase and spin reorientation in perovskite manganites. J. Magn. Magn. Mater. **491**(1), 165611 (2019). https://doi.org/10.1016/j.jmmm.2019.165611
14. M. Salamon, P. Lin, S.H. Chun, Colossal magnetoresistance is a Griffiths singularity. Phys. Rev. Lett. **88**(19), 197203 (2002). https://doi.org/10.1103/PhysRevLett.88.197203

15. M.B. Salamon, S.H. Chun, Griffiths singularities and magnetoresistive manganites. Phys. Rev. B **68**(1), 014411 (2003). https://doi.org/10.1103/PhysRevB.68.014411
16. A.K. Pramanik, A. Banerjee, Griffiths phase and its evolution with Mn site disorder in the half-doped manganite $Pr_{0.5}Sr_{0.5}Mn_{1-y}Ga_yO_3$ ($y = 0.0, 0.025$, and 0.05). Phys. Rev. B **81**(2), 024431 (2010). https://doi.org/10.1103/PhysRevB.81.024431
17. A. Silva, K.L. Salcedo Rodriguez, C.P. Contreras Medrano, G.S.G. Lourenco, M. Boldrin, E. Baggio-Saitovitch, L. Bufaical, Griffiths phase and spontaneous exchange bias in $La_{1.5}Sr_{0.5}CoMn_{0.5}Fe_{0.5}O_6$. J. Phys. Condens. Matter **33**(6), 065804 (2020). https://doi.org/10.1088/1361-648X/abc595
18. S. Thota, S. Ghosh, R. Maruthi, D.C. Joshi, R. Medwal, R.S. Rawat, M.S. Seehra, Magnetic ground state and exchange interactions in the Ising chain ferromagnet $CoNb_2O_6$. Phys. Rev. B **103**(6), 064415 (2021). https://doi.org/10.1103/PhysRevB.103.064415
19. S. Zhou, Y. Guo, J. Zhao, L. He, L. Shi, Size-induced Griffiths phase and second-order ferromagnetic transition in $Sm_{0.5}Sr_{0.5}MnO_3$ nanoparticles. J. Phys. Chem. C **115**, 1535 (2011). https://doi.org/10.1021/jp108553r
20. S. Andronenko, A.A. Rodionov, A.V. Fedorova, S.K. Misra, Electron paramagnetic resonance study of $(La_{0.33}Sm_{0.67})_{0.67}Sr_{0.33-x}Ba_xMnO_3$ ($x < 0.1$): Griffiths phase. J. Magn. Magn. Mater. **326**, 151–156 (2013). https://doi.org/10.1016/j.jmmm.2012.08.017
21. A. Kumar, R.K. Reddy, A.K. Bhatnagar, Magnetization and ESR studies of $La_{0.67}(Ca_{1-x}Mg_x)_{0.33}MnO_3$ systems. J. Alloy. Compd. **639**, 139–144 (2015). https://doi.org/10.1016/j.jallcom.2015.03.028
22. R. Eremina, I.V. Yatsyk, Y.M. Mukovskii, H.-A. Krug von Nidda, A. Loidl, Determination of the region of existence of ferromagnetic nanostructures in the paraphase of $La_{1-x}Ba_xMnO_3$ by the EPR method. JETP Lett. **85**(1), 51 (2007). https://doi.org/10.1134/S0021364007010109
23. S. Misra, S.I. Andronenko, S. Asthana, D. Bahadur, A variable temperature EPR study of the manganites $(La_1/3Sm_{2/3})_{2/3}Sr_xBa_{0.33-x}MnO_3$ (x = 0.0, 0.1, 0.2, 0.33): small polaron hopping conductivity and Griffiths phase. J. Magn. Magn. Mater. **322**(19), 2902 (2010). https://doi.org/10.1016/j.jmmm.2010.05.003
24. D.L. Huber, M.S. Seehra, Contribution of the spin-phonon interaction to the paramagnetic resonance linewidth of $CrBr_3$. J. Phys. Chem. Solids **36**(7–8), 723–725 (1975). https://doi.org/10.1016/0022-3697(75)90094-3
25. M.E. Matsnev, V.S. Rusakov, SpectrRelax: an application for Mössbauer spectra modeling and fitting. AIP Conf. Proc. **1489**, 178–185 (2012). https://doi.org/10.1063/1.4759488
26. F. Menil, Systematic trends of the ^{57}Fe Mössbauer isomer shifts in (FeOn) and (FeFn) polyhedral. Evidence of a new correlation between the isomer shift and the inductive effect of the competing bond T-X (–Fe) (where X is O or F and T any element with a formal positive charge). J. Phys. Chem. Solids **46**(7), 763–789 (1985). https://doi.org/10.1016/0022-3697(85)90001-0
27. E. Murad, J. Cashion, *Mössbauer spectroscopy of environmental materials and their industrial utilization* (Springer+Business Media, New York, 2004), p.418. https://doi.org/10.1007/978-1-4419-9040-2
28. K. De, R. Ray, R.N. Panda, S. Giri, H. Nakamura, T. Kohara, The effect of Fe substitution on magnetic and transport properties of $LaMnO_3$. J. Magn. Magn. Mater. **288**, 339–346 (2005). https://doi.org/10.1016/j.jmmm.2004.09.118
29. M. Pissas, G. Kallias, E. Devlin, A. Simopoulos, D. Niarchos, Mössbauer study of $La_{0.75}Ca_{0.25}Mn_{0.98}Fe_{0.02}O_3$ compound. J. Appl. Phys. **81**, 5770–5772 (1997). https://doi.org/10.1063/1.364722